International Journal of Pharmaceutics 392 (2010) 254–260

Contents lists available at ScienceDirect

International Journal of Pharmaceutics

journal homepage: www.elsevier.com/locate/ijpharm

Pharmaceutical Nanotechnology

Deoxycholic acid modified-carboxymethyl curdlan conjugate as a novel carrier of epirubicin: *In vitro* and *in vivo* studies

Fuping Gao[a,*,1], Lei Li[a,1], Huizhu Zhang[a,b], Wenzhi Yang[a], Hongli Chen[a], Jing Zhou[c], Zhimin Zhou[a], Yinsong Wang[d], Yuanyuan Cai[c], Xuemin Li[a], Lingrong Liu[a], Qiqing Zhang[a,e,**]

[a] *Institute of Biomedical Engineering, Chinese Academy of Medical Science & Peking Union Medical College, 236 BaiDi Road, Tianjin 300192, PR China*
[b] *Department of Pharmacology, North China Coal Medical College, 57 Jianshe Road, Tangshan 063000, PR China*
[c] *Department of Biopharmaceutics, Beijing University of Traditional Chinese Medicine, Beijing 100102, PR China*
[d] *College of Pharmacy, Tianjin Medical University, No. 22 Qixiangtai Road, Heping District, Tianjin 300070, PR China*
[e] *Research Center of Biomedical Engineering, Xiamen University, 168 DaXue Road, Xiamen, Fujian 361005, PR China*

ARTICLE INFO

Article history:
Received 30 December 2009
Received in revised form 16 March 2010
Accepted 19 March 2010
Available online 25 March 2010

Keywords:
Carboxymethyl curdlan
Deoxycholic acid
Epirubicin
Nanomedicine
Anti-tumor effect

ABSTRACT

Deoxycholic acid hydrophobically modified-carboxymethylated-curdlan (DCMC) conjugate was developed as a novel carrier for the anticancer drugs. Epirubicin (EPB), as a model drug, was physically loaded into DCMC self-assembled nanoparticles. EPB-loaded DCMC nanoparticles were almost spherical in shape and their size, in the range of 327.4–511.5 nm, increased with the EPB-loading content increasing. *In vitro* release of EPB from DCMC self-assembled nanoparticles showed sustained drug release pattern and the release rate was related to pH of release media and drug loading content. The cytotoxic activity of EPB-loaded DCMC nanoparticles was assayed by the MTT colorimetric assay. Compared with free drug, EPB-loaded DCMC nanoparticles showed the higher cytotoxicity, which may be attributed to the enhanced cellular uptake. *In vivo* toxicity study indicated that DCMC conjugate did not induce unexpected side effects. Tissue biodistribution study was performed in tumor-bearing mice. The result showed that DCMC increased the uptake of EPB in the tumor and decreased the uptake of EPB in kidney and heart, compared to free drug. Moreover, tumor volume reductions induced by DCMC conjugate, free EPB and EDNs were 24.3%, 58.9% and 70%, respectively, which suggested that EDNs could effectively retard the growth of the tumor.

1. Introduction

To improve therapeutic responses against tumors, a number of novel delivery systems, such as heparin-stabilized liposomes (Han et al., 2006), pH-sensitive polymeric micelles (Lee et al., 2005) and folic acid–conjugated dendrimeric–drug conjugate (Kukowska-Latallo et al., 2005) have been developed, recently. The nano-sized self-aggregate systems of polymeric amphiphiles composed of polysaccharides, such as pullulan (Na et al., 2003) and chitosan (Chan et al., 2007) have been developed as the carrier for the anti-tumor drugs due to the following advantages. These polysaccharide amphiphiles have been recognized as an effective strategy for passive tumor targeting (Park et al., 2006). Moreover, some polysaccharides are also known to effectively inhibit tumor growth and metastasis (Yoshitomi et al., 2004; Park et al., 2004).

Curdlan, one of the microbial polysaccharides, is a naturally occurring linear (triple helix) polysaccharide composed of 1,3-β-linked D-glucose units produced by a strain of *Alcaligenes faecalis* and mainly used as a food additive now. As reported previously (Yoshida et al., 1994; Katsuraya et al., 1994; Greinacher et al., 1995), curdlan has a potential inhibitory effect against AIDS virus infection and blood anti-coagulant activity, as well as low toxicity *in vitro* and *in vivo*. However, curdlan is insoluble in water, which limits its biological applications. Carboxymethyl substitution is considered as a method to improve the functional properties for many polysaccharides. In the case of curdlan, its carboxymethylated derivative (CM-curdlan) has good water solubility, good bioactivity as well as anti-tumor activity (Sasaki et al., 1978, 1979). We previously reported preparation and characteristics of self-assembled nanoparticles of deoxycholic acid (DOCA)-modified CM-curdlan (DCMC) (Gao et al., 2008). The hydrophobic core of these self-assembled nanoparticles was considered to act as a reservoir of hydrophobic anti-tumor drugs. In this research, epirubicin (EPB) was chosen as a model drug to assess the potential of

* Corresponding author. Tel.: +86 22 87890868; fax: +86 22 87890868.
** Corresponding author at: Institute of Biomedical Engineering, Chinese Academy of Medical Science, 236 BaiDi Road, Tianjin 300192, PR China. Tel.: +86 22 87890868; fax: +86 22 87890868.
E-mail addresses: gaofp158@gmail.com (F.-P. Gao), zhangqiq@xmu.edu.cn (Q. Zhang).
[1] Contributed equally to this work.

0378-5173/$ – see front matter © 2010 Elsevier B.V. All rights reserved.
doi:10.1016/j.ijpharm.2010.03.044

DCMC self-assembled nanoparticles as a novel carrier for the anti-tumor drugs. As an anthracycline anticancer agent, EPB has a wide range of anti-tumor activity and is used to treat various carcinomas. However, EPB therapy may cause some serious side effects such as allergic reactions, cardiotoxicity and blood problems (Cersosimo and Hong, 1986; Bonadonna et al., 1993). Therefore, DCMC self-assembled nanoparticles were used as a carrier of EPB for the purpose of sustaining its release, prolonging its circulation time, enhancing its therapeutic index and decreasing its toxic effects.

2. Experimental

2.1. Materials

Curdlan (M_W 81,000) was purchased from Wako Co. (Japan). DOCA and 1-ethyl-3-[3-(dimethylamino) propyl] carbodiimide (EDC) were purchased from Sigma Co. (St. Louis, MO, USA). N-Hydroxyl succinimide (NHS) was purchased from Aldrich Co. (Milwaukee, WI). Epirubicin (EPB) in the form of the hydrochloride salt was supplied from Hisun Pharmaceutical Co. (Zhejiang, China). 3-(4,5-Dimethylthiaol-2-yl)-2,5-diphenylterazolium bromide (MTT) was obtained from Zhongao Biotechnology Co. Ltd. (China). All other chemical reagents were analytical grade and obtained from commercial sources.

2.2. Preparation and characterization of CM-curdlan/DOCA conjugate (DCMC)

Curdlan was carboxymethylated by the method described previously (Yang et al., 2006; Zhang et al., 2004). DCMC conjugate was synthesized by coupling CM-curdlan with DOCA as described in a previous report (Gao et al., 2008). The detailed chemical structure of the DCMC is shown in Fig. 1. The DCMC was analyzed by FT-IR spectrophotometer and ^{1}H NMR (Gao et al., 2008).

2.3. Preparation and characterization of EPB-loaded DCMC nanoparticles

The EPB-loaded DCMC nanoparticles (EDNs) were prepared using an ammonium sulfate gradient method (Haran et al., 1993; Lasic et al., 1995). DCMC (20 mg) was hydrated with ammonium sulphate solution (10 ml, 0.15 M) by probe sonication, and followed by dialyzing (molecular weight cut-off 8–12 kDa) in isoosmotic solution of 0.9% NaCl solution (1000 ml) for 6 h with two exchanges to remove the free ammonium sulfate. In order to examine the effect of the different drug/carrier ratios on the entrapment efficiency and drug loading content, different amounts of EPB solution (2 mg/ml) and the plain DCMC self-assembled nanoparticles solution were mixed, and then incubated for 24 h at room temperature. The excess EPB, which was not entrapped inside the DCMC self-assembled nanoparticles, was removed by ultrafiltration using a membrane with a molecular weight cut-off of 30,000 (Amicon Centricon YM-30, Millipore, USA). Triplicate ultrafiltration was performed in this purification process. Finally, EPB-loaded DCMC self-assembled nanoparticle dispersions were freeze-dried.

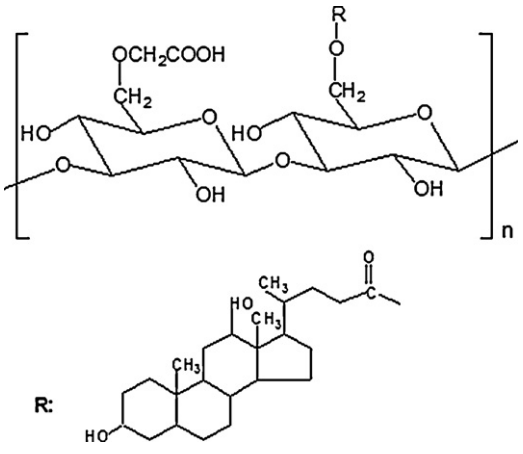

Fig. 1. Structure of deoxycholic acid (DOCA)-modified CM-curdlan (DCMC) conjugate.

The contents of EPB entrapped in the DCMC nanoparticles were determined according to the previous method (Kwon et al., 1997; Cammas et al., 1997) with a little modification using fluorescence spectrophotometer (Shimadzu RF-4500, Japan). Briefly, the EDNs solution (200 μl) was mixed with 800 μl of DMSO, and then the fluorescence intensity of EPB was measured by fluorescence spectrophotometer. The excitation wavelength (λ_{ex}) and the emission wavelength (λ_{em}) were set at 470 and 589 nm, respectively. Drug entrapment efficiencies were expressed as percentages of EPB amount in DCMC nanoparticles with respect to the initial amount of EPB used to prepare the EDNs.

The size and size distribution of EDNs in an aqueous solution were measured by dynamic light scattering (DLS) with a digital autocorrelator (Brookhaven BI-90 Plus, USA) at a scattering angle of 90°, a wavelength of 658 nm and a temperature of 25 ± 0.1 °C. DLS measurements were performed over a time period sufficient to reach equilibrium, with no evidence of change in size with time.

To observe the morphology of EDNs, the sample solution (1 mg/ml) was placed on a carbon-coated copper grid. Then, the grids were air-dried and examined using a transmission electron microscope (TEM; Tecnai G^2 20S-Twin, USA) at an accelerating voltage of 80 kV.

2.4. EPB release from DCMC nanoparticles in vitro

The drug release from EDNs was performed according to the method reported by Na et al. (2003). Freshly prepared 2 ml of EDN solutions containing same drug contents were respectively placed into the dialysis tubes (molecular weight cut-off 8–12 kDa) and then dialyzed against 10 ml of the phosphate-buffered saline (PBS) solutions with various pH (5.0, 6.5, and 7.4), or 2 ml of EDNs solutions containing different drug contents were placed in dialysis tube and dialyzed against 10 ml PBS (pH 7.4). The release test was performed at 37 °C with a stirring rate of 100 rpm. At predefined sampling time, the whole release media were exchanged with fresh media. The release amount of EPB was detected by fluorescence method above described. It should be noted that all procedures were carried out in the dark because EPB is light sensitive. The release experiment was performed in triplicate.

2.5. In vitro cytotoxicity assay

In vitro cytotoxicity of plain DCMC nanoparticles, free EPB and EDNs was assayed by MTT colorimetric assay using a human breast adenocarcinoma cell line (MCF-7). MCF-7 cells were cultured in a RPMI 1640 medium containing 10% fetal bovine serum supplemented with 100 units/ml penicillin and 100 mg/ml streptomycin at 37 °C in 5% CO_2 atmosphere. Cells harvested in a logarithmic growth phase were seeded on 96-well flat-bottomed plates at a density of 5000 cells/well and incubated for 24 h. Then, the growth media were removed from 96-well plates and 200 μl of media containing various concentrations of plain DCMC nanoparticles, free EPB and EDNs (drug loading content: 9.67%) were added. After incubation at 37 °C under a 5% CO_2 atmosphere for 24 h and 48 h, the cells were washed twice with PBS to eliminate the remaining drug and then added 100 μl of fresh culture medium and 20 μl of MTT solution (5 mg/ml in PBS) each well. After the further incubation at

37 °C for 4 h, the culture media were removed and the cells were dispersed in DMSO. Then, ultraviolet absorbance of each well at 570 nm was measured with a microplate reader (Sunnyvale, CA, USA). Each measurement of the drug concentration was obtained as the mean value of eight wells. The data are expressed as the percent of viable cells compared to control group.

2.6. Flow cytometry and confocal microscopic analysis

The extent of cellular uptake of EDNs (drug loading content: 9.67%) and free EPB was determined using a flow cytometry (Beckman coulter epics altra, USA). MCF-7 cells harvested in a logarithmic growth phase were seeded on 24 wells at a cell density of 5×10^4 cells/ml. After incubation for 24 h, the culture media containing free EPB and EDNs with the same EPB concentration of 10 μM were added, respectively. The loading amount of EPB in DCMC self-assembled nanoparticles was taken into account to adjust the EPB concentration. After further 2-h incubation, the drug-treated cells were thoroughly washed three times with PBS, and analyzed by flow cytometry. Each experiment was performed in triplicate.

The cellular uptake was visualized by a confocal microscopy (SPE-Leica, Germany). Briefly, MCF-7 cells were seeded onto cover glass pre-soaked in culture media and incubated for 24 h. Then, free EPB and EDNs with the same EPB concentration were added to the culture media. After further 2-h incubation, the cells on the cover glass were thoroughly washed three times with PBS and examined by a confocal microscopy at an excitation wavelength of 470 nm. Each experiment was performed in triplicate.

2.7. In vivo subacute toxicity of DCMC nanoparticles

In order to evaluate the safeness of DCMC self-assembled nanoparticles as a drug carrier, 24 mice (5–6 weeks old, weight: around 20 g, male C57BL/6 mouse) were randomly divided into three different groups and each group consisted of eight mice. The first group, as control, was injected 0.9% saline solution. The second group and the third group were injected DCMC self-assembled nanoparticles (2 mg/kg/3 day and 20 mg/kg/3 day; 10 times injection for each group, respectively). Each drug was injected via the lateral tail vein and body weight of each mouse was daily monitored. After 27 days, blood samples were collected via the fossa orbitalis vein for hematological and biochemistry evaluation.

2.8. In vivo distribution in tumor-bearing mice and anti-tumor activity

In the biodistribution study, a suspension of 1×10^6 cells of murine B16F10 melanoma in physiological saline (100 μl) was carefully inoculated into the subcutaneous dorsa of male C57BL/6 mice. At a predetermined time after subcutaneous inoculation, free EPB or the EDNs solution was injected into the tail vein of the tumor-bearing mice at a dose of 5 mg EPB/kg body weight. At 0.083, 0.25, 0.5, 2, 4, 8, 12 and 24 h after drug injection, each animal ($n = 5$ for each time point) was sacrificed and their heart, liver, spleen, lung, kidney and tumor as well as blood samples were collected immediately. The organs and tumor were carefully washed with ice-cold saline, blotted with paper towels to remove excess fluid, weighed and homogenized with lysis buffer (0.1 M Tris–HCl, 2 mM EDTA, 0.1% Triton X-100, pH 7.8). The lysate of each tissue and blood were centrifuged at 14,000 rpm for 20 min. The fluorescence intensity of the supernatant was measured using fluorescence spectrophotometer, as described above. The EPB concentration in each sample was determined from the net fluorescence intensity obtained by comparison with the standard curve.

In the anti-tumor activity study, subcutaneous tumors were established as above-mentioned method. Drug injection was started at 6 days after tumor inoculation and was repeated at days 9, 11, 13, and 15. Mice were allocated to four groups (six per group) as follows treatment: (i) normal saline (control group); (ii) DCMC conjugate; (iii) free EPB; and (iv) EDNs. The EPB dose administered was 5 mg/kg. Tumor volume was daily measured using calipers and was calculated using the formula, $a \times b^2/2$, where a and b were the longest and shortest diameter, respectively.

2.9. Statistical analysis

All data were expressed as mean ± S.D. and analyzed statistically using two-sample/group t-test for comparison between two different groups. For multiple comparisons of three different groups, Student's t-test was used. The level of significance was defined at $p < 0.05$.

3. Results and discussion

3.1. Preparation and characterization of EDNs

Our previous report showed that DCMC conjugate could form nanoparticles with the diameter of 192–347 nm in the aqueous media above its critical aggregation concentration and the physicochemical properties of DCMC self-assembled nanoparticles depended on the degree of substitution (DS) of DOCA (Gao et al., 2008). In this study, DCMC conjugate with DS of DOCA of 4.1 was chosen as a candidate for drug loading and further *in vivo* investigation. The anticancer drug, EPB is known as an amphiphilic weak base ($pK_a = 7.7$) due to its hydrophobic anthracycline and hydrophilic sugar moiety, and therefore the ammonium sulfate gradient method was used to prepare EDNs in this study. The ammonium sulfate gradient method is often used to load the amphiphilic weak base into the liposomes and an ammonium sulfate gradient $[(NH_4)_2SO_4]_{aggregate} > [(NH_4)_2SO_4]_{media}$ serves as a driving force in the loading process (Haran et al., 1993; Lasic et al., 1995). The characteristics of EDNs are summarized in Table 1.

As shown in Table 1, the EPB-loading content increased with the weight ratio of EPB to DCMC self-assembled nanoparticles increasing, but the entrapment efficiency decreased at the same time, which was consistent with the other reports (Lee et al., 2000; Kim et al., 2006). Table 1 also shows that the average diameter of EDNs determined by DLS increased with the increase of EPB-loading content. This suggests that EPB molecules are entrapped into the hydrophobic DCMC inner cores and the entrapped EPB molecules increase the average diameter of the DCMC nanoparticles. Considering the size and the drug loading property, we believed 1/5 (drug/carrier) was the optimal weight ratio to prepare EDNs.

Fig. 2 shows the morphology and size distribution of EDNs with a drug loading content of 9.67%. EDNs had an almost spherical shape with a unimodal size distribution and well dispersed without any aggregation. The mean diameter of these nanoparticles determined by DLS was 359.7 ± 23.7 nm, slightly larger than the size determined by TEM. As our previous report (Gao et al., 2008), the difference of EDN diameter between TEM and DLS was mainly due to the process involved in the preparation of samples. TEM depicted the size in the dried state of the sample, whereas DLS determined the size in the hydrated state of the sample.

3.2. In vitro release of EPB

In vitro release behavior of EPB from DCMC nanoparticles with different EPB loading contents in different pH media is summarized in Figs. 3 and 4. All release profiles showed a rapid release in the initial stage (phase I), and followed by a slow and sustained release,

Table 1
Characteristics of EPB-loaded DCMC self-assembled nanoparticles.

Drug/carrier[a]	Diameter[b] (nm)	Polydispersity index[b]	Loading content (%)[c]	Loading efficiency (%)[d]
1/10	327.4 ± 18.1	0.093 ± 0.012	6.56 ± 1.02	61.3 ± 5.43
2/10	359.7 ± 23.7	0.138 ± 0.021	9.67 ± 1.11	47.4 ± 4.32
3/10	359.7 ± 30.2	0.170 ± 0.019	11.77 ± 1.34	38.4 ± 3.27
4/10	511.5 ± 33.1	0.241 ± 0.020	15.83 ± 1.19	40.6 ± 4.17
5/10	583.1 ± 32.9	0.106 ± 0.017	19.26 ± 1.78	41.6 ± 3.10

[a] EPB/DCMC self-assembled nanoparticles (mg/mg).
[b] Mean diameter and polydispersity index determined by dynamic light scattering ($\theta = 90^{\circ}$) ($n = 3$).
[c] (Loading EPB/DCMC self-assembled nanoparticles) × 100% (mean value) determined by fluorescence method ($n = 3$).
[d] (Loading EPB/feeding EPB) × 100% (mean value) determined by fluorescence method ($n = 3$).

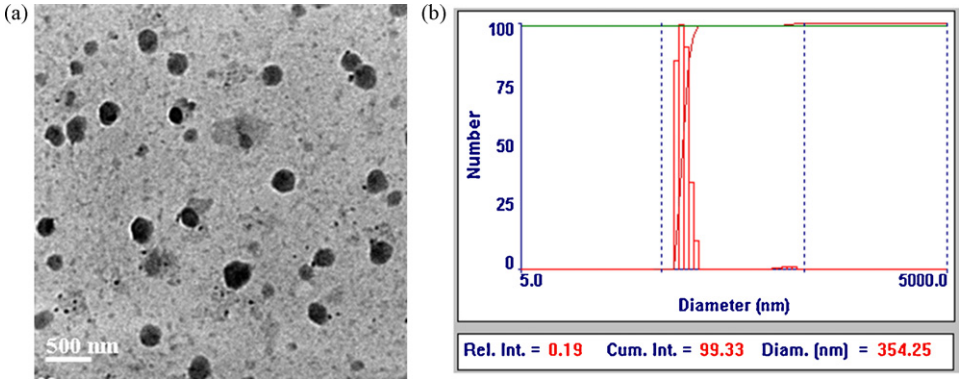

Fig. 2. TEM images and size distribution of EPB-loaded of DCMC self-assembled nanoparticles.

which seems to continue for a prolonged period of time (phase II). In general, drug release rate from the polymeric micelles depends on the solubility and diffusivity of drug. In the initial stage, the drug diffusion from the cores of nanoparticles into the outer aqueous phase was rapid due to the higher drug concentration gradient. In the later stage, the drug diffusion slowed down with the drug concentration gradient decreasing, which resulting the sustained drug release. Above result suggested that the nanoparticles might act as a barrier against the release of entrapped EPB. As shown in Fig. 3, EPB release from EDNs with EPB loading content of 9.67% was accelerated by decreasing the pH of release medium from 7.4 to 5.0. EDNs with different drug loading contents (6.56–19.26%) showed the similar release characteristics (data not shown). We believed the pH-sensitive release behavior of EPB from EDNs was mainly due to the higher solubility of EPB in the lower pH release medium, which accelerated the diffusion of EPB from DCMC nanoparticles. It has been reported that the local pH of solid tumor was one order of magnitude lower than that of normal tissue (Hoes et al., 1993; Stubbs et al., 2000), and therefore the pH-sensitive release behavior of EPB from EDNs may be advantageous for the tumor treatment. Fig. 4 shows that the higher the drug content, the slower the drug release, which was consistent with the results of other researchers (Jeong et al., 1998).

3.3. In vitro cytotoxicity

The cytotoxicity of EDNs against MCF-7 cells was evaluated using MTT assay. As shown in Fig. 5(a), the viabilities of MCF-7 cells incubated with non-drug-loaded DCMC conjugate showed high values, e.g., above 95% even at the concentration of 100 μg/ml, which indicated that DCMC conjugate did not exhibit a significant cytotoxicity against MCF-7 cells. As shown in Fig. 5(b) and (c), free

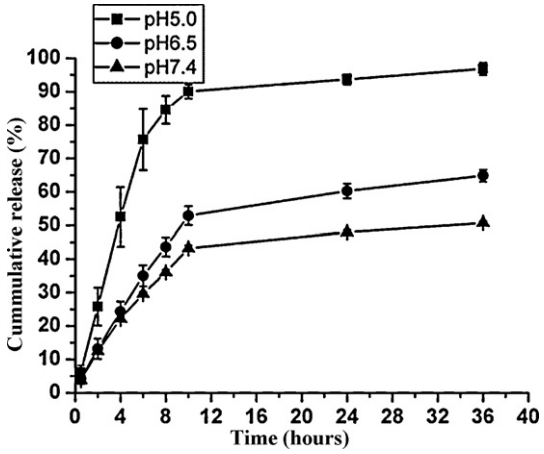

Fig. 3. Release behavior of EPB from DCMC self-assembled nanoparticals with a drug loading content of 9.67% at different pH values. Points shown are means of three replicates. Data represent the mean ± S.D.

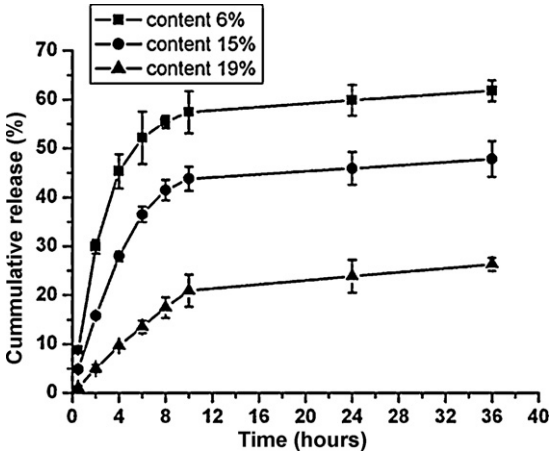

Fig. 4. Release behavior of EPB from DCMC self-assembled nanoparticals with different drug loading contents. Points shown are means of three replicates. Data represent the mean ± S.D.

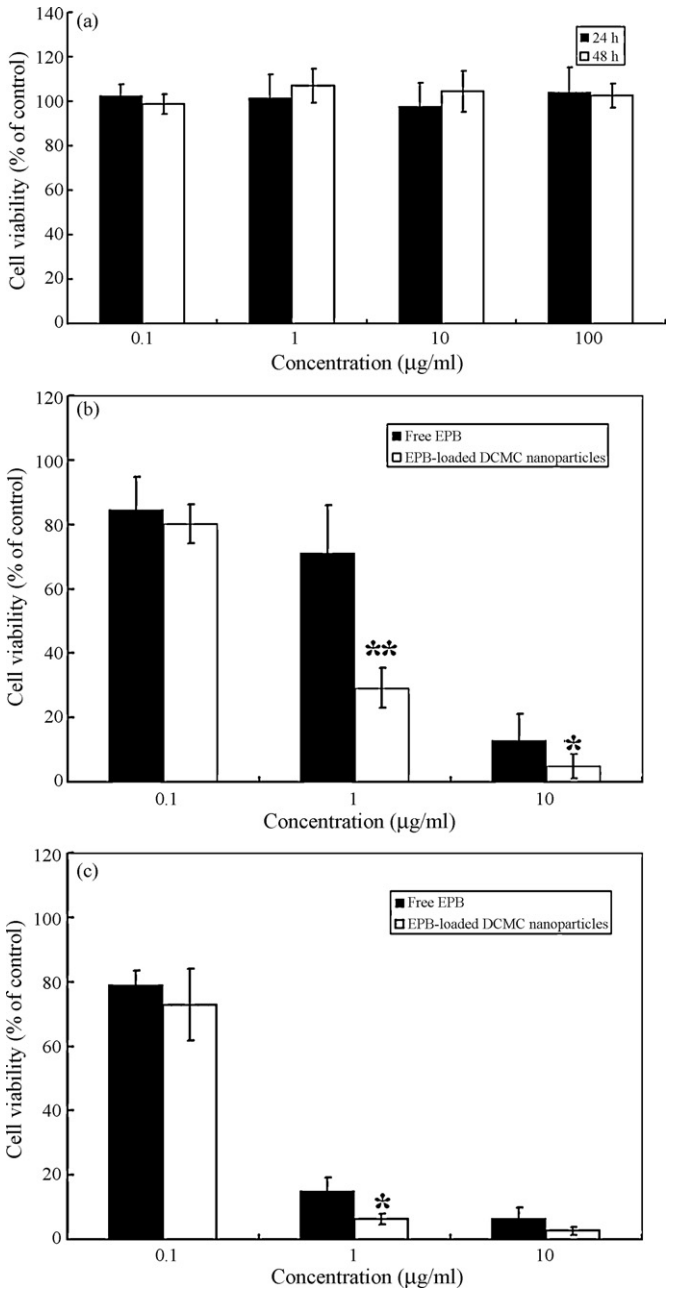

Fig. 5. Cytotoxicity of blank DCMC self-assembled nanoparticals (a) free EPB and EPB-loading DCMC self-assembled nanoparticals against MCF-7. MCF-7 cells were treated with EPB for 24 h (b) and 48 h (c) ($n = 8$, $^{*}p < 0.05$, $^{**}p < 0.01$ compared with same concentration free EPB group).

EPB and EDNs both showed the cytotoxic effect against MCF-7 cells, and this cytotoxic effect increased with the culture time up to 48 h. The inhibition of cell growth by EDNs was significantly higher than that of free EPB, especially at the concentration of 1 μg/ml (Fig. 5(b)) after incubating 24 h ($p < 0.01$).

3.4. Evaluation of cellular uptake

The uptake of free EPB and EDNs by MCF-7 cells was investigated quantitatively and qualitatively using a flow cytometry and a confocal microscopy, respectively. As shown in Fig. 6, MCF-7 cells incubated with EDNs emitted higher fluorescent intensity than those with free EPB, which suggested that the cellular uptake of EDNs was higher than that of free EPB. Confocal microscopy

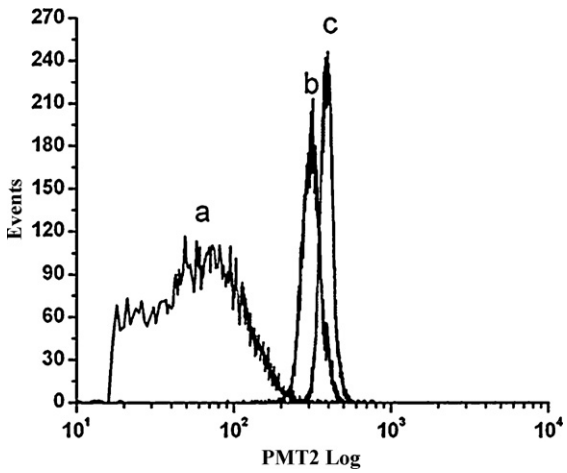

Fig. 6. Flow cytometry results of untreated MCF-7 cells (a), MCF-7 cells incubated with free EPB for 2 h (b), and MCF-7 cells incubated with EPB-loaded DCMC nanoparticles (c) with a drug loading content of 9.67% for 2 h.

also confirmed the enhanced uptake of EDNs compared to free EPB. As shown in Fig. 7, MCF-7 cells incubated with EDNs emitted more intense fluorescence than those incubated with free EPB. The enhanced uptake of EDNs by MCF-7 cells compared to free EPB could produce the higher cytotoxic effect, which was confirmed by the result of cytotoxicity *in vitro*.

3.5. In vivo subacute toxicity of DCMC nanoparticles

In order to prove the safety of DCMC conjugate as a drug carrier, we evaluated subacute toxicity of DCMC conjugate *in vivo* after repeated injection through the lateral tail vein at two doses (2 mg/kg and 20 mg/kg) for 27 days. Mice injected with DCMC conjugate at two doses showed no significant changes in body weight (Fig. 8), red blood cell, white blood cell and platelet counts (Table 2) compared to the control group. Furthermore, the levels of aminotransferases (ALT and AST), creatinine and BUN were within the normal ranges in all groups, indicating that the liver and renal functions were normal. All above results meant that DCMC conjugate did not cause the unexpected side effects and could be used as a safe drug carrier (Table 2).

3.6. In vivo distribution in tumor-bearing mice

The area under concentration curve (AUC) of free EPB and EDNs in different tissues was calculated by the trapezoid method. As shown in Fig. 9, the order of AUC from highest to lowest was liver > tumor ≥spleen > kidney > blood > heart> lung for EDNs and liver > kidney > spleen > heart ≥tumor > blood > lung for free EPB. Compared with free EPB, AUC of EDNs was significantly higher in plasma, liver and spleen ($^{*}p < 0.05$) and very significantly higher in tumor ($^{**}p < 0.01$), but significantly lower in heart and kidney ($^{*}p < 0.05$). We did not eliminated EDNs in blood was partially uptaken by the reticuloendothelial system (RES). Therefore, accumulation in spleen and liver was slightly higher with EDNs than free EPB. We believed that the higher EPB AUC of EDNs in plasma than the free EPB was due to the reduced renal excretion. Moreover, we believed that the higher EPB AUC of the EDNs in the tumor was mainly due to the enhanced permeability and retention (EPR) effect (Duncan, 1999). Brigger et al. (2002) have mentioned in their review that the cut-off size of the pores in tumor vessels is ranging between 380 and 780 nm. Direct observation of the tumor vasculature has demonstrated a tumor-dependent pore cut-off size ranging from 200 nm to 2 μm (Hashizume et al., 2000) which may permit access

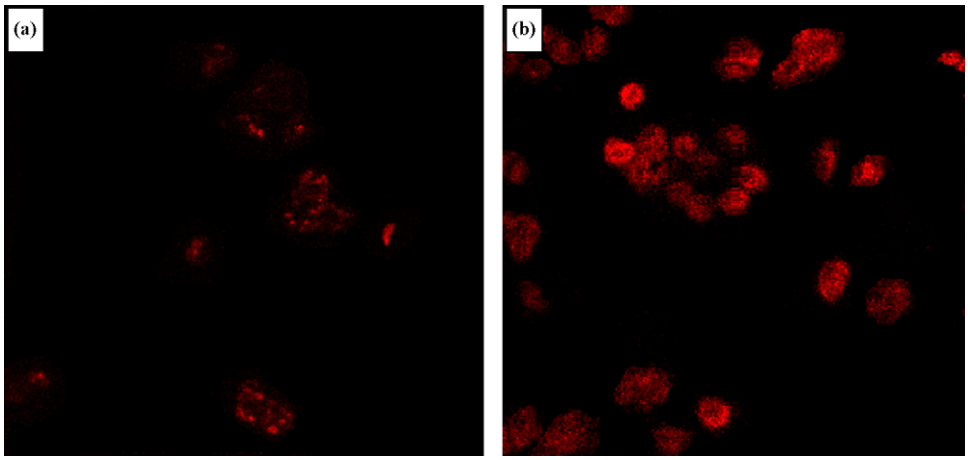

Fig. 7. Confocal microscopic images of MCF-7 incubated with free EPB (a) and EPB-loaded DCMC nanoparticles (b) with a drug loading content of 9.67% for 2 h.

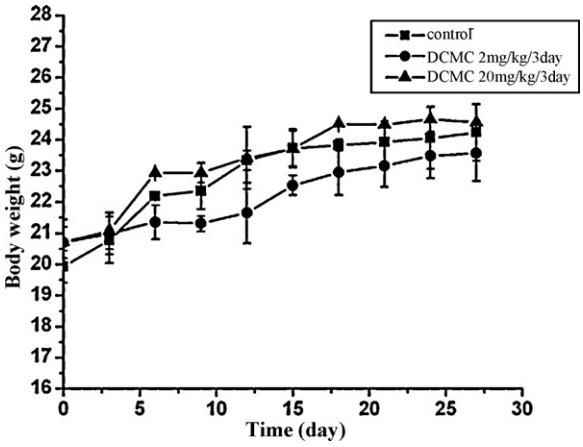

Fig. 8. Normal C57BL/6 mice body weight change after repeatedly injecting DCMC self-assembled nanoparticles. Data represent the mean ± S.D.; $n = 8$.

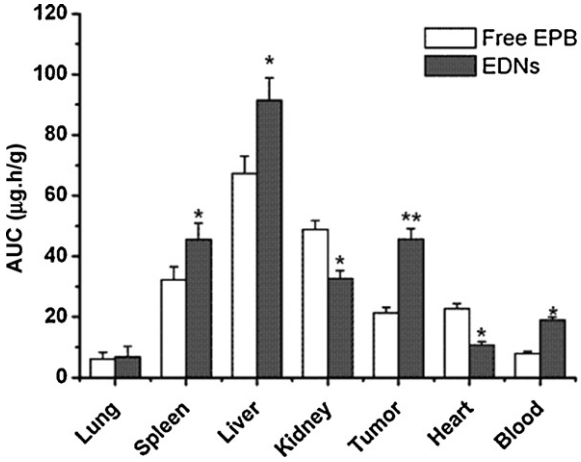

Fig. 9. Tissue distribution (AUC, 0–24 h) of epirubicin and EDNs after intravenous injection to tumor-bearing male C57BL/6 mice at the dose of 5 mg EPB/kg. Data represent the mean ± S.D.; $n = 5$ ($^{*}p < 0.05$, $^{**}p < 0.01$).

of drug-loaded nanoparticles to malignant tumor cells. Therefore, EDNs (around 350 nm in diameter) could accumulate in tumor by EPR effect. It is well known that EPB has the inherent cardiac toxicity, and therefore the reduced uptake of EPB in the heart using DCMC self-assembled nanoparticles as the carrier could reduce the severe cardiac toxicity of EPB. All above results suggested that the promising potential of EDNs to improve the therapeutic efficacy of EPB and reduce the EPB-associated systemic toxicity.

3.7. In vivo anti-tumor activity

As shown in Fig. 10, the anti-tumor activity of EDNs was determined by the change in the tumor volume. It was evident that EPB and EDNs treatments both effectively suppressed the tumor growth. But compared with free EPB, EDNs showed a more significant suppression of the tumor growth ($p < 0.05$). DCMC conjugate also mildly suppressed the tumor growth compared to the control group ($p < 0.05$). According to the reports (Sasaki et al., 1978, 1979), CM-curdlan has anti-tumor activity relating to its immunological enhancement activity. In DCMC conjugate molecule there is CM-curdlan moiety which resulted in the suppression of the tumor growth. DCMC conjugate, free EPB and EDNs induced tumor volume reductions of 24.3%, 58.9% and 70%, respectively, relative to the saline treated control. In addition to the effective accumulation of DCMC nanoparticles into the tumor tissues by EPR effect, the sustained release of EPB from DCMC nanoparticles and the immunological enhancement activity might jointly produce the more effective suppression of the tumor growth. Overall, it is evi-

Table 2
Effect of DCMC conjugate in hematology and biochemistry of normal C57BL/6 mice ($n = 8$).

	Control	DCMC conjugate (2 mg/kg/3day)	DCMC conjugate (20 mg/kg/3day)
RBC ($\times 10^6$ μl^{-1})	9.99 ± 1.23	9.47 ± 0.45	10.48 ± 0.66
WBC ($\times 10^3$ μl^{-1})	6.36 ± 1.17	7.75 ± 1.70	7.59 ± 1.61
Platelet ($\times 10^3$ μl^{-1})	221.2 ± 93.2	260.0 ± 97.7	230.2 ± 58.3
BUN (mg/dl)	20.3 ± 2.87	23.5 ± 2.16	21.4 ± 1.98
Creatinine (mg/dl)	0.32 ± 0.02	0.35 ± 0.13	0.36 ± 0.07
ALT (U/l)	18.2 ± 3.56	21.3 ± 3.12	19.8 ± 2.56
AST (U/l)	35.2 ± 8.23	33.6 ± 9.26	37.1 ± 10.21

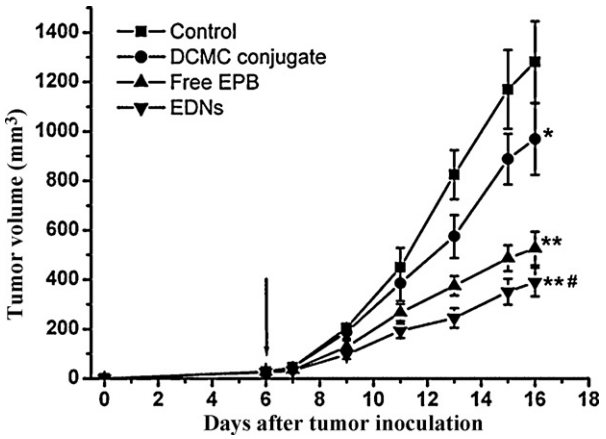

Fig. 10. Tumor growth inhibition by intravenous injection of DCMC conjugate, epirubicin and EDNs or normal saline as a control. The drug solutions were administered at 6 days after inoculation of B16F10 melanoma cells into the subcutaneous dorsa of the male C57BL/6 mice. The arrows indicate the beginning time points of the drug injection. Each point represents the mean ± S.D.; $n = 6$ ($^{*}p < 0.05$, $^{**}p < 0.01$ Compared with control group, $^{\#}p < 0.05$ Compared with free EPB group).

dent that the self-assembled nanoparticle system based on DCMC conjugate has promising potential as carrier for the hydrophobic anti-tumor drugs.

4. Conclusions

In this study, we reported a novel DOCA modified CM-curdlan (DCMC) conjugate self-assembled nanoparticles. Anticancer drugs, epirubicin (EPB) can be successfully loaded into DCMC self-assembled nanoparticles (EDNs). EDNs showed sustained drug release pattern. The *in vitro* anti-tumor activity studies using MCF-7 cells showed that EDNs were more cytotoxic than free EPB, which was ascribed to the higher uptake of EDNs compared to free EPB. *In vivo* studies indicated DCMC conjugate did not cause unexpected side effect. Tissue biodistribution study demonstrated that the self-assembled nanoparticles could improve the accumulation of EPB in tumor and reduce the uptake of EPB in the heart. The self-assembled nanoparticles loaded with EPB effectively suppressed the tumor growth *in vivo*. DCMC may be useful as a prospective carrier for anti-tumor drugs.

Acknowledgements

This study was supported by the Major State Basic Research Program of China (No. 2006 CB 933300) and the Doctoral Fund of Ministry of Education of China (No. 20060023050).

References

Bonadonna, G., Gianni, L., Santoro, A., Bonfante, V., Bidoli, P., Casali, P., Demicheli, R., Valaqussa, P., 1993. Drugs ten years later: epirubicin. Ann. Oncol. 4, 359–369.

Brigger, I., Dubernet, C., Couvreur, P., 2002. Nanoparticles in cancer therapy and diagnosis. Adv. Drug. Deliv. Rev. 54, 631–651.

Cammas, S., Suzuki, K., Sone, C., Sakurai, Y., Kataoka, K., Okano, T., 1997. Thermo-responsive polymer nanoparticles with a core–shell micelle structure as site-specific drug carriers. J. Control. Release 48, 157–164.

Cersosimo, R.J., Hong, W.K., 1986. Epirubicin: a review of the pharmacology, clinical activity, and adverse effects of an adriamycin analogue. J. Clin. Oncol. 14, 425–439.

Chan, P., Kurisawa, M., Chung, J.E., Yang, Y.Y., 2007. Synthesis and characterization of chitosan-g-poly(ethylene glycol)-folate as a non-viral carrier for tumor-targeted gene delivery. Biomaterials 28, 540–549.

Duncan, R., 1999. Polymer conjugates for tumour targeting and intracytoplasmic delivery. The EPR effect as a common gateway. Pharm. Sci. Technol. Today 2, 441–449.

Gao, F.P., Zhang, H.Z., Liu, L.R., Wang, Y.S., Jiang, Q., Yang, X.D., Zhang, Q.Q., 2008. Preparation and physicochemical characteristics of self-assembled nanoparticles of deoxycholic acid modified-carboxymethyl curdlan conjugates. Carbohydr. Polym. 71, 606–613.

Greinacher, A., Alban, S., Dummel, V., Franz, G., Muellereckhardt, C., 1995. Characterization of the structural requirements for a carbohydrate based anticoagulant with a reduced risk of inducing the immunological type of heparin-associated thrombocytopenia. Thromb. Haem. 74, 886–892.

Han, H.D., Lee, A., Song, C.K., Hwang, T., Seong, H., Lee, C.O., Shin, B.C., 2006. In vivo distribution and antitumor activity of heparin-stabilized doxorubicin-loaded liposomes. Int. J. Pharm. 313, 181–188.

Haran, G., Cohen, R., Bar, L.K., Barenholz, Y., 1993. Transmembrane ammonium sulfate gradients in liposomes produce efficient and stable entrapment of amphipathic weak bases. Biochim. Biophys. Acta 1151, 201–215.

Hashizume, H., Baluk, P., Morikawa, S., McLean, J.W., Thurston, G., Roberge, S., Jain, R.K., McDonald, D.M., 2000. Openings between defective endothelial cells explain tumor vessel leakiness. Am. J. Pathol. 156, 1363–1380.

Hoes, C.J.T., Boon, P.J., Kaspersen, F., Feijen, J., 1993. Design of soluble conjugates of biodegradable polymeric carriers and adriamycin. Makromol. Chem. Macromol. Symp. 70/71, 119–136.

Jeong, Y.I., Cheon, J.B., Kim, S.H., Nah, J.W., Lee, Y.M., Sung, Y.K., Akaike, T., Cho, C.S., 1998. Clonazepam release from core–shell type nanoparticles in vitro. J. Control. Release 51, 169–178.

Katsuraya, K., Shoji, T., Inazawa, K., Nakashima, H., Yamamoto, N., Uryu, T., 1994. Synthesis of sulfated alkyl Laminara oligosaccharides having potent anti-HIV activity and relationship between structure and biological activity. Macromolecules 27, 6695–6699.

Kim, J.H., Kim, Y.S., Kim, S., Park, J.H., Kim, K., Choi, K., Chung, H., Jeong, S.Y., Park, R.W., Kim, I.S., Kwon, I.C., 2006. Hydrophobically modified glycol chitosan nanoparticles as carriers for paclitaxel. J. Control. Release 111, 228–234.

Kukowska-Latallo, J.F., Candido, K.A., Cao, Z., Nigavekar, S.S., Majoros, I.J., Thomas, T.P., Balogh, L.P., Khan, M.K., Baker Jr., J.R., 2005. Nanoparticle targeting of anticancer drug improves therapeutic response in animal model of human epithelial cancer. Cancer Res. 65, 5317–5324.

Kwon, G., Natio, M., Yokoyama, M., Okano, T., Sakurai, Y., Kataoka, K., 1997. Block copolymer micelles for drug delivery: loading and release of doxorubicin. J. Control. Release 48, 195–201.

Lasic, D.D., Ceh, B., Stuart, M.C.A., Guo, L., Frederik, P.M., Barenholz, Y., 1995. Transmembrane gradient driven phase transitions within vesicles: lessons for drug delivery. Biochim. Biophys. Acta 1239, 145–156.

Lee, E.S., Na, K., Bae, Y.H., 2005. Doxorubicin loaded pH-sensitive polymeric micelles for reversal of resistant MCF-7 tumor. J. Control. Release 103, 405–418.

Lee, K.Y., Kim, J.H., Kwon, I.C., Jeong, S.Y., 2000. Self-aggregates of deoxycholic acid-modified chitosan as a novel carrier of adriamycin. Colloid Polym. Sci. 278, 1216–1219.

Na, K., Lee, E.S., Bae, Y.H., 2003. Adriamycin loaded pullulan acetate/sulfonamide conjugate nanoparticles responding to tumor pH: pH-dependent cell interaction, internalization and cytotoxicity in vitro. J. Control. Release 87, 3–13.

Park, J.H., Kwon, S., Lee, M., Chung, H., Kim, J.H., Kim, Y.S., Park, R.W., Kim, I.S., Seo, S.B., Kwon, I.C., Jeong, S.Y., 2006. Self-assembled nanoparticles based on glycol chitosan bearing hydrophobic moieties as carriers for doxorubicin: in vivo biodistribution and anti-tumor activity. Biomaterials 27, 119–126.

Park, S.D., Lai, Y.S., Kim, C.H., 2004. Immunopontentiating and antitumor activities of the purified polysaccharides from *Phellodendron chinese* SCHNEID. Life Sci. 75, 2621–2632.

Sasaki, T., Abiko, N., Nitta, K., Takasuka, N., Sugino, Y., 1979. Antitumor activity of carboxymethylglucans obtained by carboxymethylation of (1-3)-β-D-glucan from *Alcaligenes var faecalis myxogenes* IFO 13140. Eur. J. Cancer 15, 211–215.

Sasaki, T., Abiko, N., Sugino, Y., Nitta, K., 1978. Dependent on chair length of antitumor activity of (1-3)-β-D-glucan from *Alcaligenes var faecalis myxogenes* IFO 13140, and its acid degraded productions. Cancer Res. 38, 379–384.

Stubbs, M., Mcsheehy, P.M.J., Griffiths, J.R., Bashford, C.L., 2000. Causes and consequences of tumor acidity and implications for treatment. Mol. Med. Today 6, 15–19.

Yang, J., Zhang, H.B., Yin, Y.M., Nishinari, K., 2006. Comparison of curdlan and its carboxymethylated derivative by means of Rheology, DSC, and AFM. Carbohydr. Res. 341, 90–99.

Yoshida, T., Tasuda, Y., Uryu, T., Nakashima, H., Yamamoto, N., Mimura, T., Kaneko, Y., 1994. Synthesis and in vitro inhibitory effect of L-glucosyl-branched curdlan sulfates on AIDS virus infection. Macromolecules 27, 6272–6276.

Yoshitomi, Y., Nakanishi, H., Kusano, Y., Munesue, S., Oguri, K., Tatematsu, M., Yamashina, I., Okayama, M., 2004. Inhibition of experimental lung metastases of Lewis lung carcinoma cells by chemically modified heparin with reduced anticoagulant activity. Cancer Lett. 207, 165–174.

Zhang, M., Cheung, P.C.K., Zhang, L.N., Chiu, C.M., Ooi, V.E.C., 2004. Carboxymethylated β-glucans from mushroom sclerotium of *Pleurotus tuber-regium* as novel water-soluble anti-tumor agent. Carbohydr. Polym. 57, 319–325.